

# Synthesis, Two-Dimensional Assembly, and Surface Pressure-Induced Coalescence of Ultranarrow PbS Nanowires

Israel Patla,<sup>†</sup> Somabrata Acharya,<sup>‡,||</sup> Leila Zeiri,<sup>†</sup> Jacob Israelachvili,<sup>§</sup> Shlomo Efrima,<sup>†</sup> and Yuval Golan<sup>\*,‡</sup>

*Department of Chemistry, Department of Materials Engineering and the Ilse Katz Center for Meso and Nanoscale Science and Technology, Ben-Gurion University of the Negev, Beer-Sheva 84105, Israel, Department of Chemical Engineering, Materials Department, and Materials Research Laboratory, University of California, Santa Barbara, California 93106*

Received January 1, 2007; Revised Manuscript Received March 31, 2007

## ABSTRACT

Ultranarrow (1.8 nm) PbS nanowires are synthesized in a single step, under benchtop conditions at relatively low temperature (90 °C). The nanowires exhibit a nearly perfect crystal lattice, high width uniformity, and tight side-by-side registry. Two-dimensional (2D) assembly over large areas ( $>15 \mu\text{m}^2$ ) is achieved using the Langmuir Blodgett method. The wire width can be readily controlled in the range 1.8–10 nm by a surface pressure-induced coalescence reaction, as monitored by transmission electron microscopy and Raman spectroscopy. The fluorescence of the 2D assembly shows strong polarization dependence along the long axis of the wires, making the system potentially suitable for orientation-sensitive devices.

One-dimensional (1D) semiconductors are essential components for various applications as high-performance optoelectronic devices, field-effect transistors, logic circuits, non-volatile memories, and biosensors.<sup>1–4</sup> However, the success of such potential applications eventually depends on the quality and control over the nanowire composition and morphology. Lead sulfide (PbS) quantum particles are a class of unique materials that are extremely important for both basic scientific studies and technological applications. The large exciton Bohr radius (20 nm) owing to the nearly equal contribution from electrons and holes allows an enhanced level of quantum confinement, giving advantages over II–IV or III–V type materials.<sup>5</sup> From a technological perspective, PbS is an extremely promising material for a large number of applications in the mid- and near-infrared emission and detection range,<sup>6</sup> biological applications,<sup>7</sup> and

optoelectronic devices.<sup>8,9</sup> There has been great interest recently in PbS nanocrystals of various shapes.<sup>10–13</sup> However, relatively larger sizes of the PbS nanomaterials hampered the desired levels of quantum confinement. In a single study on ultranarrow PbS nanowire composites grown within Na-4 mica channel templates,<sup>14</sup> reported “breaks and gaps” and the use of a template could severely limit potential application of these nanowires.

Here we report on a simple route for the production of uniform, ultranarrow (1.8 nm) single-crystal PbS nanowires, 100–120 nm in length, with tight control over their width, two-dimensional (2D) distribution, and assembly. To our knowledge, this is the first approach to produce such ultranarrow PbS wire assemblies by direct chemical synthesis. The ultranarrow width of the wires is manifested in their absorption, photoluminescence (PL) and Raman spectroscopy. We further demonstrate controlled assembly of the nanowires into 2D ultrahigh-density nanowire arrays over an area of  $15 \mu\text{m}^2$  using the Langmuir Blodgett (LB) technique. Control over the nanowire thickness by side-by-side coalescence is demonstrated by varying the applied 2D surface pressure,  $\Pi$ . Finally, the 2D LB films exhibit strong anisotropic optical properties in polarized PL, which is noteworthy for optoelectronic applications.

\* To whom correspondence should be addressed. E-mail: ygolan@bgu.ac.il.

<sup>†</sup> Department of Chemistry and the Ilse Katz Center for Meso and Nanoscale Science and Technology.

<sup>‡</sup> Department of Materials Engineering and the Ilse Katz Center for Meso and Nanoscale Science and Technology.

<sup>§</sup> Department of Chemical Engineering, Materials Department, and Materials Research Laboratory, University of California.

<sup>||</sup> Present address: International Center for Young Scientists, National Research Institute for Materials Science, 1-1 Namiki Tsukuba, Ibaraki 305-0044, JAPAN.

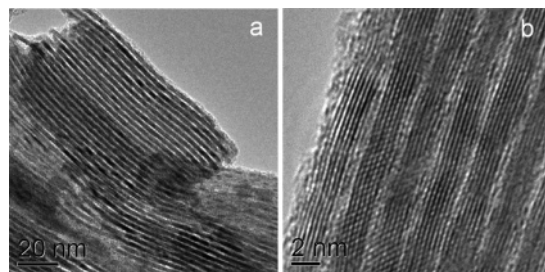


**Figure 1.** (a) TEM and (b) HRTEM images of ultranarrow PbS wires self-assembled into 2D supercrystalline arrays.

The synthesis makes use of trioctylamine (TOA), a liganding solvent that enables a single step, benchtop low-temperature decomposition of lead hexadecylxanthate, a single precursor, producing PbS nanowires.<sup>15</sup> Reaction conditions result in crystalline, rocksalt PbS, and the coordinating solvent TOA enables 1D growth, as previously shown for ZnO nanowire growth.<sup>16</sup> The capping ligand plays an important role in determining the nanocrystal shape and size in addition to stabilizing the particles. Usually, the presence of the amine moiety induces 1D growth and affects the supercrystalline nature of the nanomaterial.<sup>17–19</sup> It is anticipated that with its higher nucleophilic nature, TOA should be bound to the lead ions in the inorganic core of the nanowire, similar to other amines used for capping of nanocrystalline semiconductors (see for example refs 18 and 20).

Transmission electron microscopy (TEM) images of TOA-coated PbS wires of  $1.8 \pm 0.08$  nm diameter are shown in Figure 1a,b. The ultrathin wires are self-assembled into 2D supercrystalline arrays without any postsynthesis treatment over an area of  $0.02 \mu\text{m}^2$  by simply putting a drop of suspension ( $\sim 10 \mu\text{L}$ ) from a microsyringe onto a transmission electron microscopy (TEM) grid, maintaining the ultranarrow width and tight side-by-side registry. The center-to-center lateral distance (pitch) between the nanowires is measured to be  $2.7 \pm 0.1$  nm, which is less than the upright alkyl tails of two TOA molecules (2.44 nm, calculated from the geometry of the stretched chains) indicating tilting and/or interpenetration of the TOA tails. High-resolution TEM (HRTEM) (Figure 1b) shows that the wires are single crystalline with well-resolved lattice planes parallel to the length of the wires with an interplanar spacing of  $0.29 \pm 0.03$  nm, consistent with the (200) d-spacing of the PbS rocksalt crystal structure. Energy-dispersive sepectrometry (EDS) analysis carried out in the TEM (Supporting Information, Figure S1) gives a Pb to S molar ratio of  $\sim 1:1$ , in line with a stoichiometric crystal. The rocksalt structure of the wires is further verified by selected area electron diffraction (SAED) and powder X-ray diffraction (XRD) (Supporting Information, Figures S2 and S3).

The calculated ratio of actual wire radius/exciton Bohr radius is  $0.045 \pm 0.005$  suggesting a very strong degree of confinement. The strong quantum confinement is indeed reflected in the absorption and PL spectra (Supporting Information, Figure S4). The absorption spectrum shows three bands at 520 nm (2.39 eV), 325 nm (3.83 eV), and 290 nm (4.29 eV). All bands are due to exciton absorption

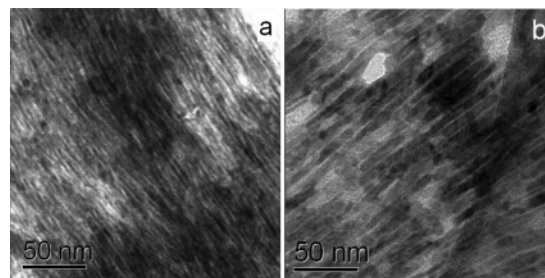


**Figure 2.** TEM images showing (a) large scale assembly of PbS wires at  $\Pi = 23$  mN/m and (b) thicker wires after coalescence at  $\Pi = 25$  mN/m for 90 min.

corresponding to  $1S_c \leftarrow 1S_h$ ,  $1S_c \leftarrow 1P_h$ ,  $1P_c \leftarrow 1P_h$  transitions, respectively,<sup>21</sup> and all are blue-shifted due to strong quantum confinement. The PL spectrum shows a strong band-edge emission at 480 nm. Deconvolution of the spectrum reveals a second peak at 500 nm and a weak, low-energy peak at 665 nm. Typical quantum yield of the wires measured relative to Coumarin 480 dye was 1.5%. Our spectral features appeared at higher energies compared with previous reports,<sup>21,22</sup> indicating a higher degree of quantum confinement.

The advantage of the LB technique for inducing nanowire alignment on a large scale into 2D assemblies in a single step (without additional postdeposition treatment for patterning) has now been well established.<sup>20,23–25</sup> The 2D supercrystalline nature of surfactant-coated PbS wires makes them excellent candidates for large scale building blocks for LB assembly. At zero or low surface pressure, the nanowires are arranged in random domains with a relatively large separation between them.<sup>20</sup> However, within each individual domain, the nanowires are highly ordered and maintain inherent 2D supercrystalline structure. The uniaxial compression irreversibly aligns the nanowire domains with their long axis parallel to the barrier. The best alignment was achieved at surface pressures in the range of 22–25 mN/m with good end-to-end and side-by-side registry. We are able to align the PbS wires into areas exceeding  $15 \mu\text{m}^2$  (Figure 2a; for a larger scale image see Supporting Information, Figure S5). To our knowledge, this is the largest area reported to be patterned by a 2D technique with an ultrahigh-pitch density (2.7 nm) that is well below the limit of conventional lithography. The compressed layer can be transferred in a single step to a variety of substrates (glass, quartz, gold, etc.) by LB deposition with a transfer ratio close to unity to yield large scale parallel nanowires. Additionally this process of assembly formation is flexible to fabricate complex networks to yield ultrahigh-density junctions well-below the lithographic limit.<sup>20</sup> Moreover, a variety of three-dimensional heterojunctions of different band gap materials can be directly achieved using this technique simply by changing the composition in each step of the deposition.

Interestingly, application of higher surface pressure of 30 mN/m (close to the collapse pressure) for 60–90 min at ambient temperatures (22 °C) clearly induces a side-by-side coalescence reaction,<sup>26</sup> resulting in thicker wires (6–10 nm) while retaining the same rocksalt structure. The end-to-end

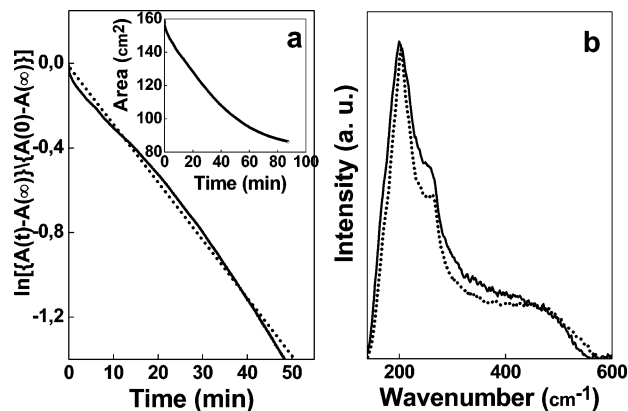


**Figure 3.** (a) First-order kinetic analysis of the area versus time decay curve. Inset: decay curve at constant surface pressure of 25 mN/m. The dotted line denotes the linear fit of the kinetic analysis. (b) Raman spectra with 632.5 nm excitation for three-layer LB films of 1.8 nm wires (solid curve) and 8–10 nm thicker wires (dotted curve).

registry for these thicker wires in the long range assembly is observed to be broken more frequently. In addition to the applied surface pressure, which is of the order of a few tens of megapascals within the Langmuir film, the ultranarrow side-by-side separation ( $\sim 0.8$  nm) between the nanowires in adjacent rows and the low melting point of TOA are supportive for the coalescence phenomena observed. The coalesced nanowires obtained were monocrystalline in nature, as shown by TEM lattice images (HRTEM) in Supporting Information, Figure S6.

The rate of coalescence is obtained from the decrease in monolayer area with time (Figure 3a, inset) set at  $\Pi = 25$  mN/m. The area reduction is measured to be 44%, in line with the TEM images of Figure 2a,b, suggesting coalescence of 3–5 ultranarrow wires into one wider wire. We carry out the first-order kinetics analysis from the decay curve using the relation

$$k(T) = [A(t, T) - A(\infty, T)] / [A(0, T) - A(\infty, T)]$$

where  $A(t, T)$  is the monolayer area measured at time  $t$ ,  $A(\infty, T)$  is the asymptotic area measured after the reaction at 22 °C set at  $\Pi = 25$  mN/m, and  $k(T)$  being the rate constant. The analysis (Figure 3a) suggests that the coalescence reaction follows first-order kinetics with a rate constant  $k(T)$  of  $0.027 \text{ min}^{-1}$  at 22 °C. The energy required to remove a TOA moiety from the nanowire surface can be estimated based on the applied surface pressure and area reduction during coalescence.<sup>26</sup> The activation energy,  $E_a$ , calculated using the relation  $k(T) = \chi \exp(-E_a/kT)$  with  $\chi$  being the frequency factor<sup>26</sup> is several  $k_B T$  per TOA molecule, in reasonable agreement with recent density functional theory calculations carried out for a similar, yet not identical system.<sup>27</sup> Direct calculation of the energy required for removing a TOA molecule from a cross-section of two coalescing wires at  $\Pi = 25$  mN/m assuming removal of 10 molecules per coalescing pair gives a similar value of several  $k_B T$ . This surface pressure-aided coalescence process carried out at ambient temperature thus enables control over nano-

wire thickness. Application of elevated surface pressure combined with elevated temperature is anticipated to yield also 2D nanosheets in a similar fashion. Both the thin and thicker wire arrays can be readily transferred onto a variety of solid supports as LB films, allowing for their use in technological applications.

Interestingly, the coalescence into thicker wires by surface pressure is reflected in the Raman spectra of LB films lifted onto 50 nm thick evaporated gold substrate<sup>28</sup> before and after coalescence (Figure 3b). The exciton–phonon coupling via Fröhlich interaction of vibrational modes and their overtone appear at  $200 \text{ cm}^{-1}$  ( $lp = 0$ ) and  $466 \text{ cm}^{-1}$ .<sup>29</sup> Significant narrowing of the  $200 \text{ cm}^{-1}$  band is observed for the  $\sim 8$  nm wide wires lifted after coalescence. The LB films consisting of 1.8 nm wires lifted before coalescence showed considerable broadening in comparison to the  $\sim 8$  nm coalesced wires, as expected for a higher degree of confinement with a smaller width.

Notably, the PL spectra of the LB films (five layers) lifted on glass substrate show strong polarization dependence in a direction parallel to the long axis of the nanowires. We have used a fluorometer (Fluorolog, Jobin Yvon) with excitation and detection polarizers in the input and output pathways. For each data, two sets of measurements were performed to extract the polarization ratio ( $r$ ). In the first set, the excitation polarizer was rotated from 0 to 180° (from parallel to parallel setting with the wires). In the second set, the excitation polarizer was rotated from 90 to 270° (from perpendicular to perpendicular setting with the wires). In each measurement, the detection was done from 0 to 180° (parallel emission). This process allows cross-polarization excitation at each point and corresponding detection. The most intense spectrum clearly appeared with parallel polarizer settings for both excitation and detection. The  $\sim 480$  and 500 nm emission bands were strongly polarized in a direction parallel to the nanowires, respectively. The lowest energy (665 nm) low-intense emission band was also polarized in the same direction, but to a much lesser degree. The polarization ratio was determined by rotating the excitation polarizer along a pair of angles with respect to the LB film with simultaneous detection of the emission angle (inset of Figure 4). The polarization ratio  $r$  for the nanowires was found to be  $0.76 \pm 0.02$  by fitting the intensity ratio  $r = (I_{\parallel} - I_{\perp}) / (I_{\parallel} + I_{\perp})$  versus detection angle with a sine function. Here  $I_{\parallel}$  and  $I_{\perp}$  are the intensities parallel and perpendicular to the long axis of the nanowires, respectively, (inset of Figure 4). Through the use of the same polarization setup, the nanowire suspension also showed polarization, but to a lesser degree of  $0.28 \pm 0.02$ , which further decreased upon diluting the suspension concentration. This degree of polarization in solution probably originates from the presence of submicron-sized ordered domains of nanowires, as shown in Figure 1a. However, the degree of polarization is less due to ensemble averaging. The high polarization ratio within the LB films reflects a high degree of orientation of the nanowire superstructures. Single-particle spectroscopy experiments are underway and are expected to yield even higher polarization due to avoidance of ensemble averaging. The PL polarization dependence



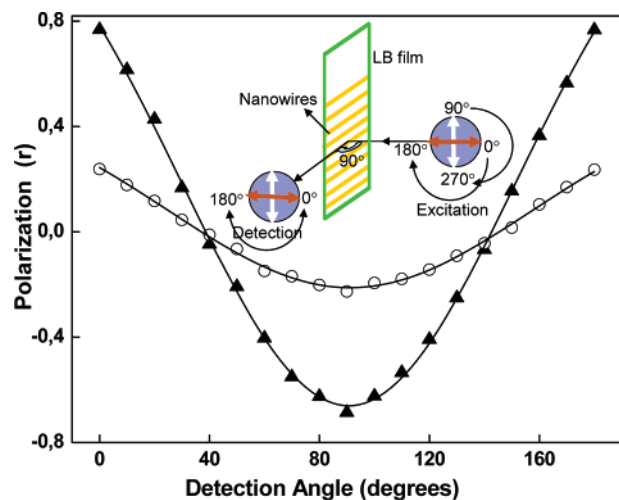


**Figure 4.** Polarization angle resolved PL spectra of the organized LB films (5 layers,  $\Pi = 23$  mN/m,  $T = 22$  °C) lifted onto glass slide (triangles) show strong polarization dependence in parallel direction, as monitored at  $\sim 480$  nm emission. The gain of the LB trough feedback loop was kept at the minimum value during deposition after reaching the surface pressure of 23 mN/m to prevent side-by-side coalescence of the wires. The spectrum obtained for a nanowire suspension (the same used for spreading onto the Langmuir trough surface) also showed some degree of parallel polarization yet to a lesser extent of 0.28 (circles), which further decreased upon diluting the concentration of the suspension. The inset shows a scheme of the polarization measurement setup.<sup>17</sup> The polarization directions are denoted with respect to the laboratory frame of reference and the applied electric field (which determines the direction of the major axis of the ordered nanowires in the LB film) with 90° being vertical and 0° is horizontal.

along the long axis is in-line with previous reports on CdS nanowires,<sup>17</sup> InP nanowires,<sup>30</sup> and CdSe nanorods.<sup>31,32</sup> Such LB films of highly anisotropic nanowire assemblies have important potential for polarization sensitive optical device applications.

In summary, we have reported on a simple route for the production of uniform and ultranarrow PbS nanowires. Long-range (over  $15 \mu\text{m}^2$ ) ordering of the nanowires in 2D by the LB technique has been demonstrated. Control over the width of the nanowires has been achieved by surface pressure-induced side-by-side coalescence. In principle, this technique can be used to achieve more complex patterns that can find potential use in a large variety of applications.

**Acknowledgment.** This work was supported by the US–Israel Binational Science Foundation, Grant No. 2002059.

**Supporting Information Available:** EDS, SAED, XRD, absorption and PL of wires, TEM of large scale LB assembly, and HRTEM. This material is available free of charge via the Internet at <http://pubs.acs.org>.

## References

- (1) Cui, Y.; Zhong, Z.; Wang, D.; Wang, W. U.; Lieber, C. M. *Nano Lett.* **2003**, *3*, 149.
- (2) Huang, Y.; Duan, X.; Cui, Y.; Lauhon, L. J.; Kim, K.-H.; Lieber, C. M. *Science* **2001**, *294*, 1313.
- (3) Patolsky, F.; Zheng, G.; Hayden, O.; Lakadamyali, M.; Zhuang, X.; Lieber, C. M. *Proc. Natl. Acad. Sci. U.S.A.* **2004**, *101*, 14017.
- (4) Melosh, N. A.; Boukai, A.; Diana, F.; Gerardot, B.; Badolato, A.; Petroff, P. M.; Heath, J. R. *Science* **2003**, *300*, 112.
- (5) Kang, I.; Wise, F. W. *J. Opt. Soc. Am. B* **1997**, *14*, 1632.
- (6) Bakueva, L.; Konstantatos, G.; Levina, L.; Musikhin, S.; Sargent, E. H. *Appl. Phys. Lett.* **2004**, *84*, 3459.
- (7) Bakueva, L.; Gorelikov, I.; Musikhin, S.; Zhao, X. S.; Sargent, E. H.; Kumacheva, E. *Adv. Mater.* **2004**, *16*, 926.
- (8) Schaller, R. D.; Petruska, M. A.; Klimov, V. I. *J. Phys. Chem. B* **2003**, *107*, 13765.
- (9) Lu, W.; Fang, J.; Ding, Y.; Wang, Z. L. *J. Phys. Chem. B* **2005**, *109*, 19219.
- (10) Lee, S.; Jun, Y.; Cho, S.; Cheon, J. *J. Am. Chem. Soc.* **2002**, *124*, 11244.
- (11) Hines, M. A.; Scholes, G. D. *Adv. Mater.* **2003**, *15*, 1844.
- (12) Li, J.; Cao, X. *J. Phys. Chem. B* **2006**, *110*, 184.
- (13) Joo, J.; Na, H.; Yu, T.; Yu, J. H.; Kim, Y. W.; Wu, F.; Zhang, J. Z.; Hyeon, T. *J. Am. Chem. Soc.* **2003**, *125*, 11100.
- (14) Mukherjee, P. K.; Chatterjee, K.; Chakraborty, D. *Phys. Rev. B* **2006**, *73*, 035414.
- (15) Leadhexadecylxanthate (0.07g.) was added under  $\text{N}_2$  to 2 ml of tri-octylamine (98%) at 60 °C with continuous stirring. When a grayish milky color appeared, the temperature was increased to 90 °C. Annealing was carried for 90 min at this temperature to complete the reaction. Finally, the temperature was reduced to 70 °C (for 15 min), and the wires were harvested (at 70 °C) by washing three times with methanol (centrifuge at 3000 rpm for 3 min) and then with a mixture of dichloromethane and methanol (1:9 by volume).
- (16) Yuhas, B. D.; Zitoun, D. O.; Pauzauskie, P. J.; He, R.; Yang, P. *Angew. Chem., Int. Ed.* **2006**, *45*, 420.
- (17) Acharya, S.; Patla, I.; Kost, J.; Efrima, S.; Golan, Y. *J. Am. Chem. Soc.* **2006**, *128*, 9294.
- (18) Panda, A. B.; Acharya, S.; Efrima, S. *Adv. Mater.* **2005**, *17*, 2471.
- (19) Panda, A. B.; Glaspell, G.; Samy El-Shall, M. *J. Am. Chem. Soc.* **2006**, *128*, 2790.
- (20) Acharya, S.; Panda, A. B.; Belman, N.; Efrima, S.; Golan, Y. *Adv. Mater.* **2006**, *18*, 210.
- (21) Machol, J. L.; Wise, F. W.; Patel, R. C.; Tanner, D. B. *Phys. Rev. B* **1993**, *48*, 2819.
- (22) Peterson, J. J.; Krauss, T. D. *Nano Lett.* **2006**, *6*, 510.
- (23) Tao, A.; Kim, F.; Hess, C.; Goldberger, J.; He, R.; Sun, Y.; Xia, Y.; Yang, P. *Nano Lett.* **2003**, *3*, 1229.
- (24) Jin, S.; Whang, D.; McAlpine, M. C.; Friedman, R. S.; Wu, Y.; Lieber, C. M. *Nano Lett.* **2004**, *4*, 915.
- (25) Yang, P. *Nature* **2003**, *425*, 243.
- (26) Acharya, S.; Efrima, S. *J. Am. Chem. Soc.* **2005**, *127*, 3486.
- (27) Rempel, J. Y.; Trout, B. L.; Bawendi, M. G.; Jensen, K. F. *J. Phys. Chem. B* **2006**, *110*, 18007.
- (28) Golan, Y.; Margulis L.; Rubinstein, I. *Surf. Sci.* **1992**, *264*, 312; **1992**, *273*, 460.
- (29) Krauss, T. D.; Wise, F. W. *Phys. Rev. B* **1997**, *55*, 9860.
- (30) Wang, J.; Gudiksen, M. S.; Duan, X.; Cui, Y.; Lieber, C. M. *Science* **2001**, *293*, 1455.
- (31) Hu, J.; Li, L.; Yang, W.; Manna, L.; Wang, L.; Alivisatos, A. P. *Science* **2001**, *292*, 2060.
- (32) Rothenberg, E.; Ebenstein, Y.; Kazes, M.; Banin, U. *J. Phys. Chem. B* **2004**, *108*, 2797.

NL070001Q